

The M-DAW Project

Investigations in Novel Wing Tip Device Design

A Mann*

Airbus, Bristol, BS99 7AR, UK

Dr. Ing. E Elsholz†

Airbus, Bremen, 28199, Germany

The M-DAW Project (Modelling and Design of Advanced Wing tip devices) aims to deliver to the European aerospace industry a novel wing tip device concept to improve aircraft efficiency and thus environmental impact together with an improved capability to accurately predict the effect of wing tip device design on aircraft performance. This paper describes the approach taken within M-DAW to investigate the potential for additional aircraft performance benefits from novel devices including an extensive review of the state of the art. Some current results are presented. The first phase of the project undertook detailed wind tunnel investigations of wing tip device aerodynamics. Both low speed and high speed, high Reynolds number testing was performed on a common wing with three datum tip devices characterising current state of the art technology. In addition to force measurements and extensive pressure measurements, wake data was obtained during both tests at cryogenic temperatures. At low speed in the DNW-KKK wind tunnel facility a PIV (Particle Image Velocimetry) system was employed and at high speed in the ETW facility an innovative DGV (Doppler Global Velocimetry) system was developed and applied to obtain qualitative wake measurements at high Reynolds numbers. The results have been used to confirm and develop the understanding of wing tip device aerodynamics and provided extensive data for CFD validation. Design studies are reported covering a variety of novel devices and a regular review process is described, enabling an estimation of the performance benefits during the design process. The project aims to conclude with the demonstration of a chosen novel device via high Reynolds number wind tunnel tests.

Nomenclature

C_L	Lift Coefficient
C_D	Drag Coefficient
C_{Mroll}	Rolling Moment Coefficient
L/D	Lift over Drag Ratio
Re	Reynolds Number
C_p	Pressure Coefficient
q/E	Ratio of Dynamic Pressure to Modulus of Elasticity
WRBM	Wing Root Bending Moment

I. Introduction

IT has been estimated that since the beginning of civil jet transportation aircraft fuel efficiency has improved by 70%, of which 30% has been due to advances in the airframe design and 40% due to engine technology. With continuing market demands and growing awareness of the environmental impact of aviation the drive to improve remains. A report by the Intergovernmental Panel on Climate Change in 1999¹ highlighted a number of emerging

* Wing Shape Specialist, Aerodynamics Design and Data, Airbus UK, New Filton House, 7DO

† Aerodynamic Design Methods, Airbus D GmbH, Huenefeldstrasse 1-5

technologies that have the potential to further reduce aircraft environmental impact. One item identified was advanced wing tip device design, which can deliver benefits in reducing emissions at all phases of a flight and can reduce community noise by improving aircraft efficiency during take-off and landing. A key advantage of this technology is that it can be retrofitted onto existing aircraft products subject to structural limits at relatively little cost. Thus there is the potential for environmental improvements ahead of the long term replacement of aircraft with service lives of over 25 years. More recently the Strategic Research Agenda² prepared by ACARE (Advisory Council for Aeronautical Research in Europe) set the direction for European research to fulfil the European Aeronautics Vision for 2020. This Vision defines challenging targets for improvements in the affordability, environmental impact, safety, operational efficiency, and the security of air transport. The Vision 2020 objectives, such as 50% cuts in CO₂ emissions and perceived noise, represent a step change in performance and have focused more attention on novel concepts. Once again advanced wing tip devices were identified as having the potential of offering a contribution in the short term.

The M-DAW Project³ (Modelling and Design of Advanced Wing tip devices) was launched in 2002 with the aim to deliver to the European aerospace industry a novel wing tip device concept to improve aircraft efficiency and thus environmental impact together with an improved capability to accurately predict the effect of wing tip device design on aircraft performance.

The objectives of this project are to: *develop a deeper understanding of the aerodynamics* of conventional wing tip devices through wind tunnel testing at high and low speed; *assess the capabilities of advanced CFD* to predict the effect of these devices by benchmarking against the experimental results; exploit the enhanced understanding to *explore novel wing tip device concepts* through the application of CFD and finally to *demonstrate* the most promising device by wind tunnel testing to determine the benefit on future aircraft products and derivatives.

II. Induced Drag

A. Induced Drag Theory and Design Practise

Lift is generated through a net imbalance of pressure above and below a wing. The pressure distribution across the span of a finite 3D lifting system results in spanwise components to the flow that differ between the upper and lower surfaces and so impart a rotational component behind the trailing edge. This is particularly strong at the extreme end of a lifting surface, where high pressure lower surface flow curls up and around the tip and creates a distinct tip vortex. These tip vortices dominate the wake system, creating the classic horseshoe vortex system. The bound and trailing vortex system introduces a downward velocity component into the aircraft wake.

Induced drag is the drag resulting from the generation of lift through these vortex systems and may be understood in a number of ways. Based on simple lifting line theory it may be described as the component of the lift force pointing aft due to the downwash behind the wing, since the lift vector is defined as being normal to the flow direction. It may also be understood in terms of the translational and rotational kinetic energy lost into the wake or as a component of pressure drag coming from the net pressure difference in the longitudinal direction on a lifting surface induced by the trailing vorticity.

The classic formulation for induced drag describes an inverse relationship with wing aspect ratio and a dependence on the wing spanwise lift distribution. Using lifting line theory it is possible to demonstrate the classic result that an elliptic distribution of load across the wing span, results in a constant spanwise downwash and gives the minimum induced drag possible, but it is important to note that this is strictly for an unswept planar wing. A further result of lifting line theory is Munk's stagger theorem which states that the total induced drag of a lifting system is not changed when the elements are moved in the streamwise direction, suggesting that wing sweep has no impact. This is a purely inviscid result for planar systems and does not account for viscous vortex roll-up characteristics and non-planar wakes.

In aircraft design the induced drag must be balanced with other constraints. Often the optimum solution for an aircraft may not incorporate an elliptic load distribution since this could require a heavier structure to support the outer wing loads, implying a high wing weight equating to an increase in drag. Additionally for transonic aircraft outer wing loads must be constrained to ensure acceptable wave drag levels and buffet performance.

For a given lift requirement an optimum planar wing solution may be found which manages the loads efficiently without the need for a special device at its tip. Many aircraft designs, however, are constrained in span rendering the optimum planar wing impractical from a ground handling perspective. Non-planar solutions, incorporating tip devices, can compensate for these geometric limitations by an increase in the effective span, and thus effective aspect ratio. That is: the distance between the wing tip vortices and thus the size of the aircraft wake can be different for wings of the same geometric span. In some cases derivative aircraft based on existing airframes can take advantage from tip devices as relatively cheap additions to move the wing towards an optimum solution for changed

requirements. In all cases it remains essential to carefully manage the loads, balancing pure aerodynamic benefits with the structural implications.

As for induced drag, the operation of conventional tip devices can be understood from several perspectives. Due to the local flow field at a wing tip the lift vector of a conventional winglet will point forward creating a negative drag force, i.e. thrust, that more than compensates for the additional wetted surface. Alternatively one can consider the net benefit from reduced energy losses within a lower momentum wake, either due to a reduced downwash or improved diffusion of the tip vorticity.

B. Approaches to Induced Drag Reduction

A state of the art review was performed at the beginning of the M-DAW project to collate existing approaches to the reduction of induced drag. This review covered references from early end-plate experiments by Prandtl to the current industrial experience of Airbus and recent patents for future tip devices.

Swept, tapered and crescent planform extensions have been proposed since the 1920's. Benefits have been claimed either due to the non-planar wake behind the wing at incidence or a thrust force component on the leading edges of a swept tip. If the sweep of the tip is larger than the wing flexural axes the device may also impact aeroelastic behaviour at high loads. The Boeing 1991-2000 raked tip patents^{4,5} claim benefits through this mechanism, demonstrating the multi-disciplinary nature of the tip design problem.

Light aircraft and UAV's sport a wide variety of wing tip shapes, many based on flow physics described in early 1949 studies by Hoerner who considered the impact on the tip vortex roll-up mechanism, suggesting that an increased effective span is possible by moving the tip vortex core further outboard.

In 1954 R Vogt was granted a patent⁶ on a twisted wing fin that sought to exploit a thrust component of the lift generated on an aerodynamic surface mounted within the vortical tip flow. One might regard this as the first winglet design. This was refined in the R T Witcomb 1976 examination⁷ of a double element swept winglet leading to an application on the MD-11 in 1990. The Boeing 747-400 received a retrofitted winglet device in 1988, whilst the Airbus A340/A330 and McDonnell Douglas C-17 incorporated winglets into the aircraft from entry into service. Recent developments have resulted in proposals for increasingly blended winglets, such as the shark fin device, a patent for which was granted to G Heller in 2004⁸. The shark fin is a highly blended non-planar wing tip extension gaining additional advantage from conical sweep.

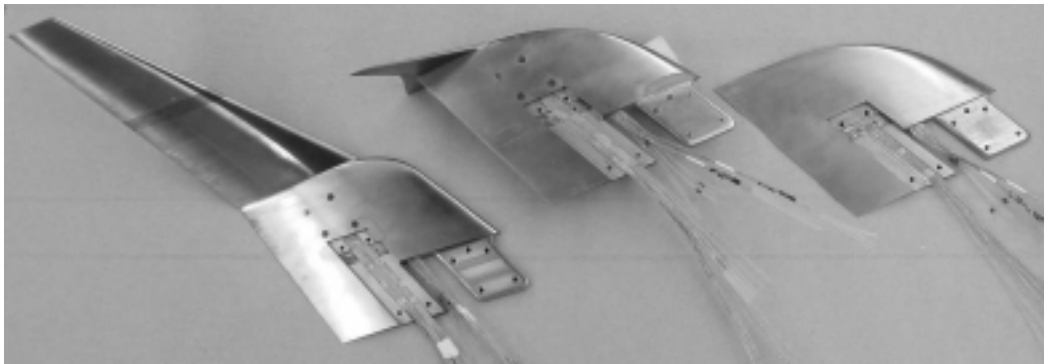


Fig. 1 M-DAW Datum Wing Tip Devices for the ETW High Speed Model (Winglet, Fence, Küchemann)

A novel embodiment of the winglet is the Airbus wing tip fence described in a 1987 patent⁹ by J Jupp and P Rees, which generates non-planar lift using stable vortical flow from a small delta wing at the wing tip. This device will not suffer stall as readily as an attached flow winglet and the impact on wing bending moment is extremely small. It has been used on the Airbus A300/A310, and A320 aircraft as well as the new A380 airliner. They prove particularly useful for retrofits since the impact on wing load is small, and are employed on the span limited A380 to give an effective wing span which is optimum for the aircraft.

The split tip device or tip sails are an extension of the basic winglet concept incorporating two or more tandem vanes. Additional advantage has been claimed due to the multiple wakes and improved vortex dispersal.

Spiroid devices¹⁰ are being developed by L Gratzler of Aviation Partners Inc. Reductions in fuel consumption of over 10% have been claimed following application to a Gulfstream II in 1992. The device consists of a looped aerodynamic surface at the wing tip with the aim of avoiding the concentrated tip vortex. In recent years C-wings have been suggested, where a further inboard canted element is attached to a winglet tip, enabling novel

management of the wing loads. Finally an extensive category of wing tip devices that claim to remove the tip vorticity entirely have been considered since the 1930's, the most recent example being the Hugues 2002 patented helical slotted tube¹¹, which claims to reduce induced drag by 8%.

The survey of concepts revealed that in wing tip design there is little new under the sun. Current successful devices, and most of the unsuccessful or unproven devices, can be traced back in various forms to the early days of powered flight. The aerodynamic mechanisms exploited in the successful designs are in fact limited to either the reduction of vortex core intensity, dispersing the wake vorticity more rapidly, or the increase of vortex core spacing often through non-planar devices, to increase effective aspect ratio.

The chosen datum devices are a large canted winglet and an Airbus tip fence (Fig. 1). Relative to a normal swept Küchemann tip these devices represent two extremes. The large winglet, whilst relatively lightly loaded, adds a significant bending moment penalty to a wing and may imply an increase in geometric span. It does however provide significant drag improvement at both high and low speed. The wing tip fence has a lower gain in simple drag terms but brings a substantially lower weight penalty with no geometric span increase and thus may prove a better option depending on the aircraft.

III. Experimental Investigation

A. Experimental Overview

The investigation of current wing tip technologies centred on extensive wind tunnel test campaigns to analyse the flow physics of two conventional devices in greater depth than has been achieved previously. The aims were three-fold, each contributing to one of the prime objectives of M-DAW. Through advanced measurement techniques the current understanding of wing tip device aerodynamics was strengthened, a high quality database was established providing detailed data for CFD validation, and a challenging baseline performance was demonstrated against which any novel device will be compared. Tests were performed both at high transonic speed and at low speed at the ETW and DNW-KKK cryogenic facilities respectively during 2003.

The project made use of existing half-models, representing a research wing geometry used in previous European research projects, most notably HiReTT¹². Both high and low speed models represent a large four-engined transonic civil airliner and embody the same wing shape enabling a single aircraft scenario to be studied. The basic wings incorporated swept Küchemann tips, used as the baseline, and allowed for the attachment of alternative tips, enabling the study of the M-DAW datum conventional devices, a large canted winglet and an Airbus tip fence.

In addition to force measurements both tests incorporated extensive pressure measurements, including pressure tappings on the wing tip devices themselves, and measurement of the wake immediately behind the wing tip.

B. Low Speed Results

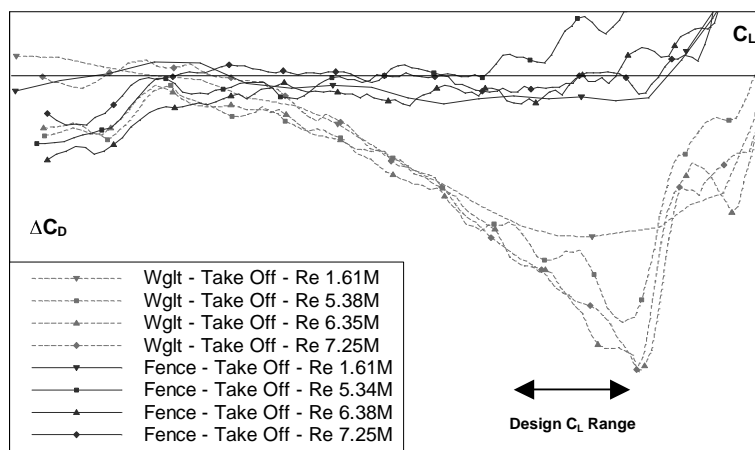


Fig. 2 Mach 0.2 DNW-KKK Tip Device Incremental Drag Relative to the Küchemann Wing for different Reynolds Numbers on the Take-Off Configuration

The low speed tests were conducted in the DNW-KKK atmospheric pressure tunnel at Mach 0.2 over a range of Reynolds numbers from 3.4 million up to 7.3 million at cryogenic temperatures. The model had installed through-

flow nacelles, and incorporated deployable high lift devices. All three tip devices were tested, the baseline Küchemann, the large canted winglet and the tip fence, each on both the Clean configuration and a representative Take-Off configuration with deployed slats and flaps.

Only small differences were seen with varying Reynolds number in terms of basic drag performance as is evident in Fig. 2. There are clear differences in the stall behaviour of the winglet as Reynolds number changes however. At winglet stall where load is lost on the winglet the drag benefit dramatically reduces. This indication of winglet $C_{L,max}$ can be seen to occur at higher wing C_L 's as Reynolds number increases, as may be expected.

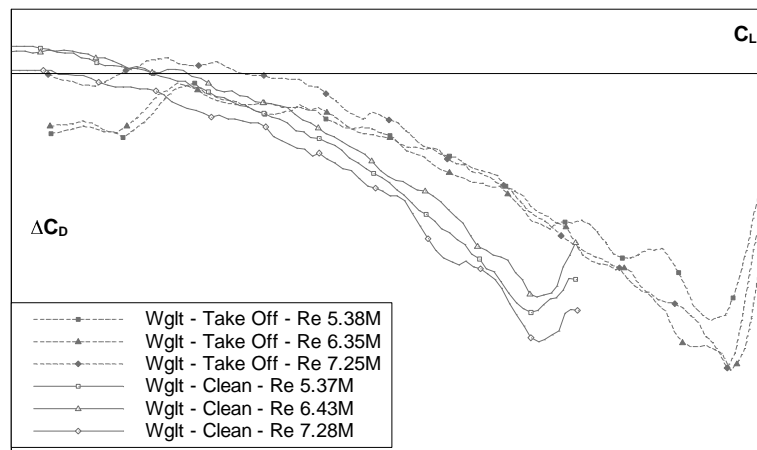


Fig. 3 Mach 0.2 DNW-KKK Incremental Drag Relative to the Küchemann Wing for the Winglet on the Clean and Take-Off Configurations

With flaps deployed the load distribution over the wing span tends to become more inboard biased. This creates less cross flow over the tip region and thus any tip device will experience less load and generate less drag reduction for a given C_L . This trade is seen in Fig. 3 where winglet drag increments for Clean and Take-off configurations are presented. The winglet curve is shifted to the right for the Take-Off case since a higher wing C_L is required to provide the winglet with the same onset conditions. During low speed aircraft operation different slat and flap settings will be applied for different lift requirements. The resulting changes in tip flow tend to be favourable for the winglet, which thus remains below its stall point across the wing C_L range at low speed. A comparison of the fence and winglet devices demonstrates the value of span for low speed performance. In low speed design it is also important to recognise the effect of the slats, which, though they do not affect the span load, do increase wing $C_{L,max}$ and thus may require the winglet to operate at higher loads by effectively shifting the design condition.

C. High Speed Results

The high speed tests were conducted in the ETW tunnel over a range of Mach numbers from 0.70 to 0.89, at Reynolds numbers from 25 million up to 70 million based on a.m.c. (close to flight conditions) and temperatures from 194 K down to 115 K. The datum Reynolds number for this model, where the wing reaches its high speed design twist, is 54.2 million. Due to the tunnel's ability to independently control pressure and temperature it was possible to isolate the effect of Reynolds number and load. By controlling the tunnel conditions the ratio of dynamic pressure to the model's modulus of elasticity, q/E , was kept constant enabling a range of Reynolds numbers to be tested on a constant wing shape.

Figure 4 plots the drag increments measured for the winglet and fence devices relative to the Küchemann device over a range of Reynolds numbers for a given q/E , and thus constant wing twist for a given C_L . Changes in the increments for the different Reynolds numbers, whilst larger than expected from simple theory, are generally within the tunnel repeatability and invariant with C_L .

The effect of span loading can be seen in Fig. 5 where drag increments at a constant Reynolds number are plotted for varying q/E . A high q/E and thus wing load results in greater wing bending and thus increased twist-off which moves the span loading inboard relative to the design Reynolds condition. It is clear that lower outboard loading reduces the effectiveness of a tip device, which operates at a lower load due to the reduced cross flow at the tip.

The associated penalties of the devices can be represented in Fig. 6 in the plot of incremental rolling moment. Data is plotted again for different wing twist shapes at the design Mach number and Reynolds number. Not only is the winglet's effect on wing bending moment evident, but also its variation with wing twist which is far more pronounced than that for the fence. Thus it is seen that, whilst the fence offers less drag reduction, the resulting structural impact is relatively insensitive to C_L and wing loading when compared to a large attached flow device.

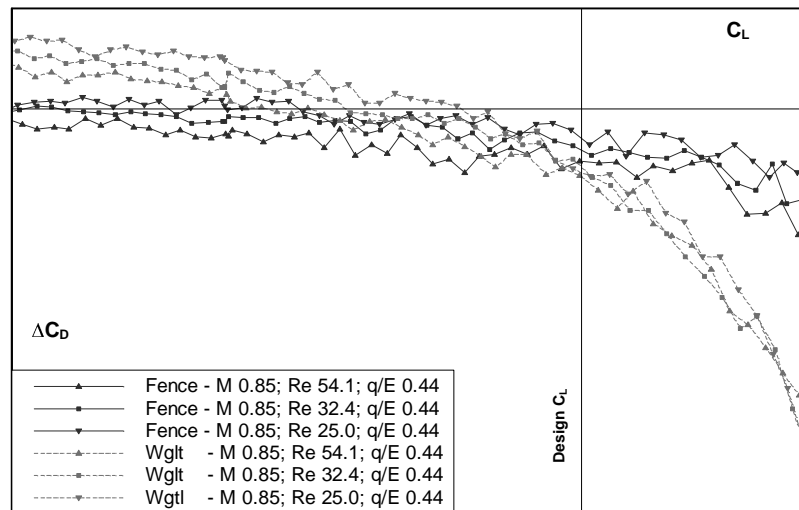


Fig. 4 Mach 0.85 ETW Tip Device Incremental Drag Relative to the Kuchemann Wing for 3 Reynolds Numbers at constant q/E

The M-DAW half model used in ETW is extensively pressure plotted, having 7 stations of sectional pressure tappings on the basic wing, plus some tappings on the tip devices and in the tip junction. In addition to CFD validation these may be used to infer a twist deformation during the test. ETW processed the pressure data and based on variations with wing incidence estimated an incremental wing twist plotted in Fig. 7.

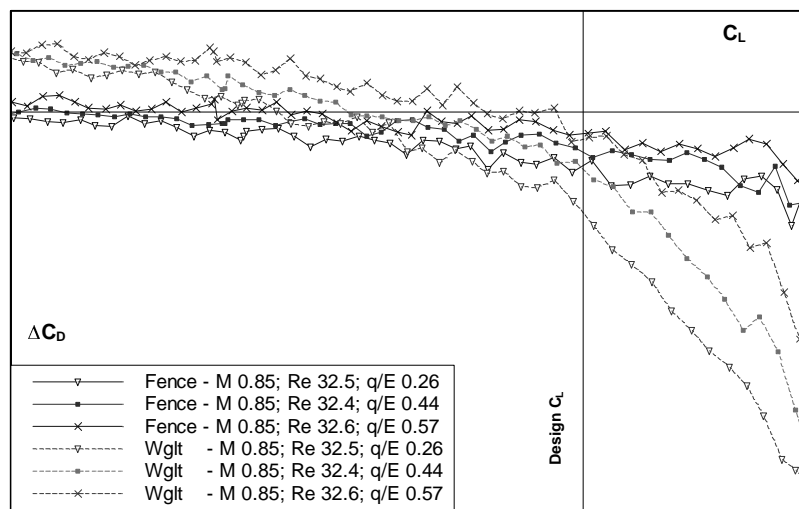


Fig. 5 Mach 0.85 ETW Tip Device Incremental Drag Relative to the Kuchemann Wing for 3 q/E values at constant Reynolds Number

The impact of the additional load on wing twist due to the winglet is clear. It is to be noted that the wing was designed for a Kuchemann tip only and thus the addition of a winglet has moved the wing away from its design shape. If the twist-off is not accounted for the trades above demonstrate that the winglet will be operating below its intended load.

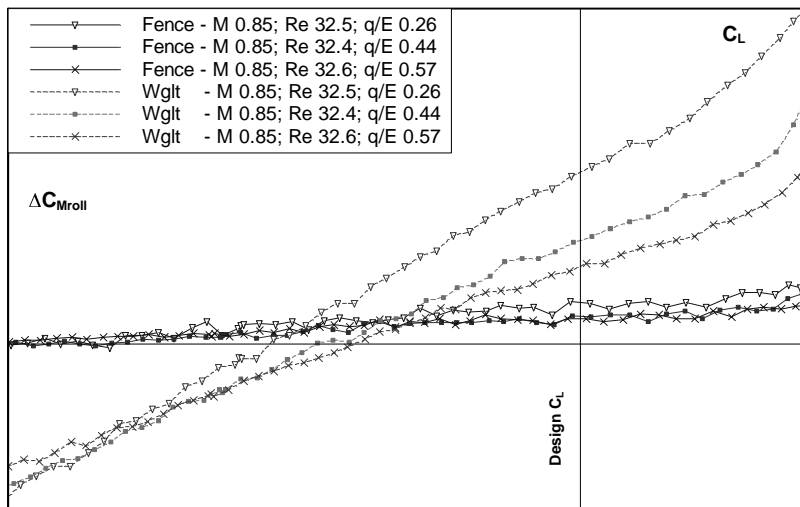


Fig. 6 Mach 0.85 ETW Tip Device Incremental Rolling Moment Relative to the Kuchemann Wing for 3 q/E at constant Reynolds Number

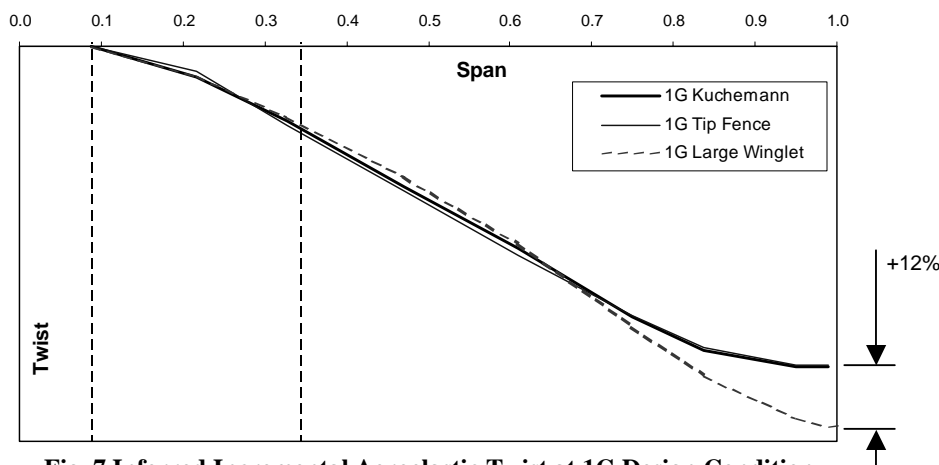


Fig. 7 Inferred Incremental Aeroelastic Twist at 1G Design Condition

D. Wake measurements

Both tests incorporated measurements of the wake behind the wing tip. The low speed tests applied the PIV (Particle Image Velocimetry) Technique at cryogenic conditions for the first time. For the high speed tests a new DGV (Doppler Global Velocimetry) system was developed and applied in ETW, providing a unique dataset and capability within Europe. The techniques and their application within the M-DAW project are given a full treatment in a paper by C Willert of DLR et al.¹³.

The PIV technique uses a double-pulsed laser light sheet to illuminate a seeded flow. The double exposures are analysed to determine the component velocities normal to the mean tunnel flow from the displacement of particle images. A low concentration of seeding is required for this approach and thus dispersed oil was used for the M-DAW low speed tests providing 1 μ m particles up to a density of 10 particles/mm³. It has been estimated that less than 1ml of oil entered the tunnel during the entire test campaign. Pulsed laser light optics were mounted directly onto the outside of the tunnel wall. The time delay between laser pulses varied around 7-20 μ s. The camera was mounted in a heated housing on a traversable sting behind the model in the tunnel flow. It was equipped with a remote rapid focusing lens to accommodate the temperature-induced changes in refractive index as the tunnel

temperature was reduced down to 100 K. PIV measurements were taken at the lowest temperature and thus highest Reynolds number. The field of view achieved with this system was $84 \times 112 \text{ mm}^2$ though this was increased to $250 \times 200 \text{ mm}^2$ after merging of several views taken with the traversing sting.

Figure 8 gives an example of the data obtained with the PIV system in the M-DAW DNW-KKK low speed tests. The wakes, plotted as vorticity contours, behind the three tip configurations at a low incidence are superimposed indicating the relative positions of the vortex cores. This data has been used to validate numerical wake models and study the relative strengths of the wake vorticity with the aim of identifying the major sources of drag.

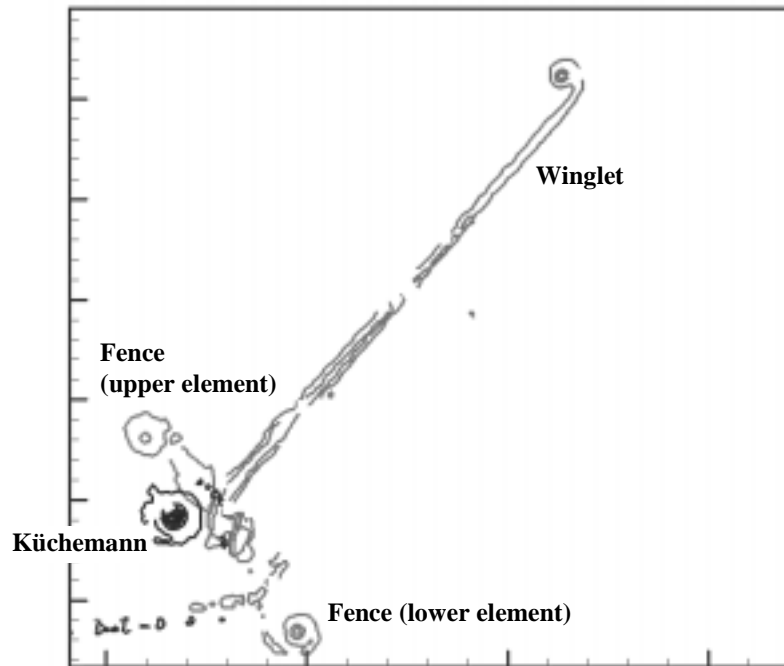


Fig. 8 DNW-KKK PIV Image Behind the Large Winglet Device at Mach 0.2

The installation of a wake measurement system in ETW posed various challenges that resulted in the use of a different technique. The test section is inaccessible, being enclosed in a pressure vessel, and thus any equipment must be controlled remotely and operate at pressures up to 4.5 bar and cryogenic temperatures down to 110 K. In addition the camera equipment cannot be located in the high speed tunnel flow as for the low speed PIV measurements. Finally, due to the costs associated with running the tunnel, data acquisition must be rapid.

This set of constraints and requirements led to the choice of a DGV system optimised for the measurement of time averaged velocity data. DGV measures velocity components indirectly through measurement of the frequency shift of light scattered in the particles of a seeded flow. The seeding required is of a greater luminosity and higher density than that for PIV. The solution adopted for the ETW DGV system was the injection of warm nitrogen and water vapour just behind the working section of the tunnel. This mixture undergoes sublimation in the dry cryogenic atmosphere of the tunnel, immediately forming tiny ice crystals. Continuous injection of about 1Kg/s dry nitrogen mixed with saturated steam was necessary to avoid a gradual decay in luminosity due to the continuous blow off in the ETW tunnel.

The seeded flow is illuminated with a laser sheet formed by a sweeping beam. By tuning the laser light onto a transitional slope of a molecular absorption band a frequency shift in the light results in a change of light intensity transmitted through the molecular absorber. Iodine vapour provides the molecular absorption band, a cell of which is placed in front of a CCD camera. A second CCD reference camera is given the same signal ahead of the iodine cell by means of a beam splitter. The measured Doppler shift is related to the laser light direction and observation direction, thus a single view and laser sheet provides a single velocity component. In order to measure three component velocities the system developed in M-DAW used two co-planar laser sheets and a three view arrangement. Rather than building three separate camera systems fibre optic bundles were used to carry the three

signals from the tunnel walls to a single camera system. The three views plus a reference image used to monitor the laser frequency were merged into a common image consisting of four quadrants. The camera system was packaged into a thermally insulated heated enclosure.

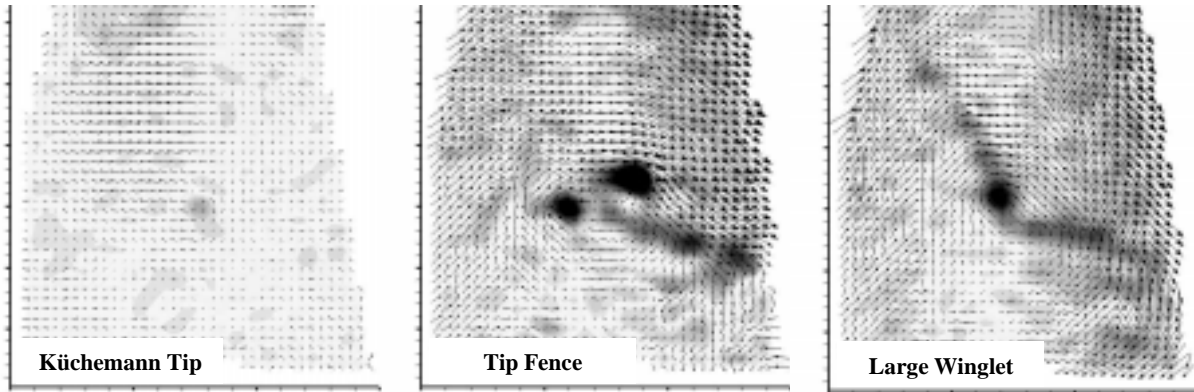


Fig. 9 ETW DGV Image Behind the Küchemann Tip, Fence and Large Winglet Devices at Mach 0.85

To test the system and the seeding technique a mock campaign was carried out ahead of the M-DAW tests. This measured the wake behind two vortex generators and provided invaluable experience in the use of DGV in ETW. In particular areas of the tunnel working section walls were painted in dull black paint following this trial run to avoid signal contamination from scattered light. The M-DAW test campaign itself demonstrated the reliability of the innovative and complex systems and identified further areas for development. The technique used for particle generation resulted in some ice accretion on wind tunnel wall windows at certain conditions during wake measurements, which along with the use of fibre optic cables gave some loss in signal intensity. The resulting DGV

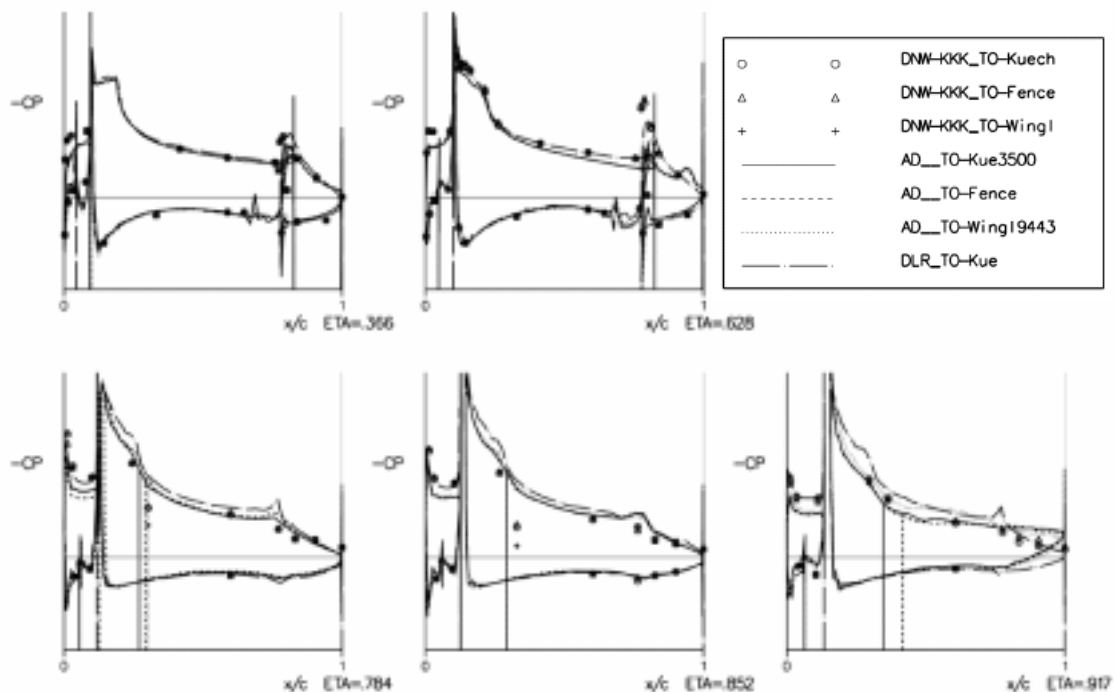


Fig. 10 Low Speed Wing Pressures, WTT & CFD, Take-Off Config, Mach 0.2, α 11°, Re 7million

data required smoothing and was not suitable for quantitative analysis, though the images remained useful for CFD validation. Figure 9 gives images behind all three devices tested at the design Reynolds number a little above the design C_L . The DGV measurements were performed separately from force and pressure measurements to avoid any impact on data quality.

IV. Validation of Numerical Methods

An important aspect of the project was the demonstration of numerical methods in the design and analysis of wing tip devices. Thus an extensive validation exercise has been undertaken making use of the experimental data to both prove aerodynamic CFD tools and aid further understanding of tip device aerodynamics.

A. Low Speed

The low speed model incorporated pressure tapings on the wing, high lift devices and tip devices enabling detailed validation of the numerical methods. Figure 10 provides a comparison at high incidence, plotting Navier-Stokes results with the measured data for wing pressures on the take-off configuration. The data includes all three tip devices though their impact on the wing pressures is seen to be negligible in comparison to the numerical grid dependency.

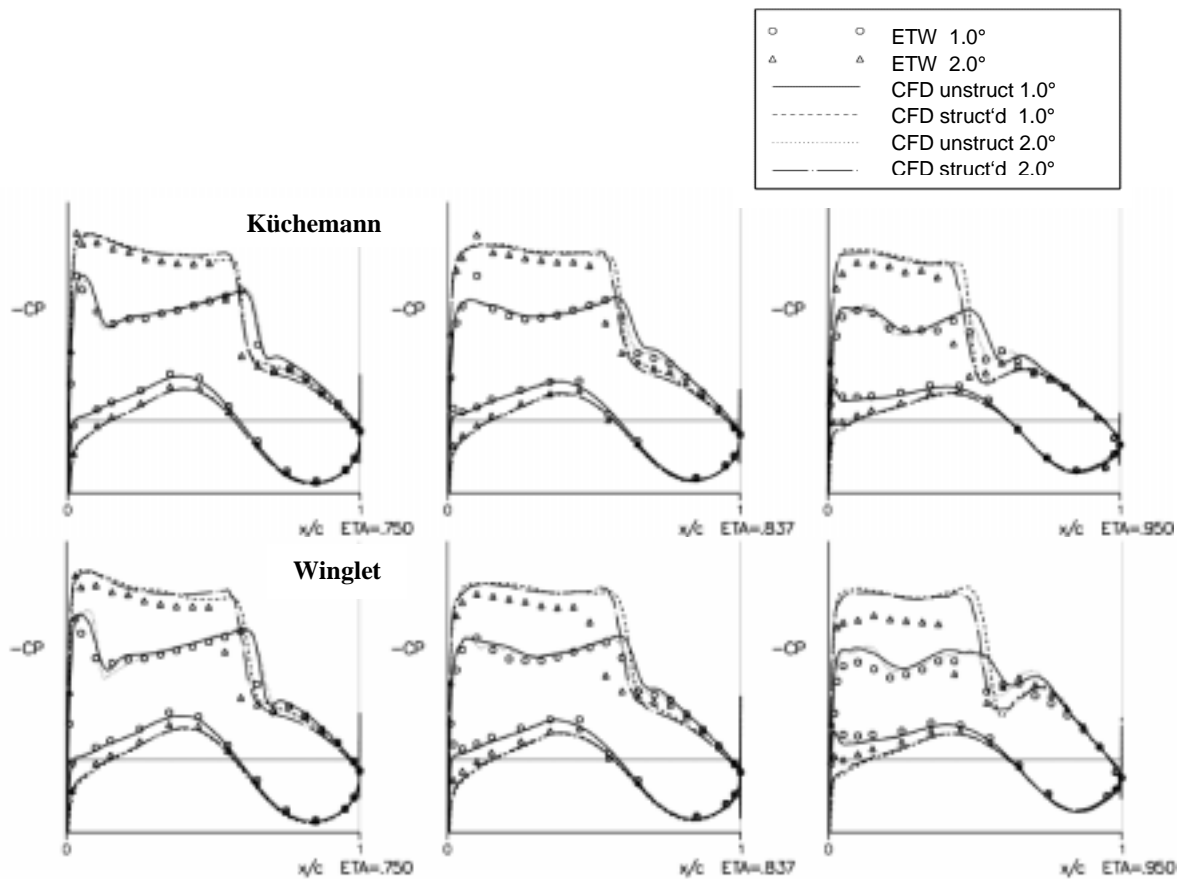


Fig. 11 Outboard Wing High Speed Pressures, WTT & CFD, Mach 0.85, Re 54.2million

B. High Speed

A comparison of measured and Navier-Stokes predicted pressures is also given for the high speed model in Fig. 11. The cases shown are for the Küchemann and Winglet configurations at the design Mach No. for two incidences either side of the design lift, for the outboard wing only. The fence configuration is not included here since it makes a negligible difference to the wing pressures except in the local tip junction. The wing pressures are shown to

develop rapidly with incidence around the design point requiring accurate prediction of the lift curve slope to obtain satisfactory pressure comparisons at a given C_L . It also becomes vital to understand the aeroelastic behaviour of the model in order to correctly model the wing twist. The winglet configuration in particular displays a significantly different twist as noted above in Fig. 7 and thus significantly different outer wing pressure distributions as seen in Fig. 11. The CFD predictions are based on the 1G design wing shape with no device attached. The aeroelastic impact of the winglet is the dominant effect over the wing.

Measured and predicted pressures in the wing tip junction region and on the devices themselves are plotted in Fig. 12. CFD is seen to capture the major effects, though the importance of capturing the aeroelastic impact of the winglet is again indicated.

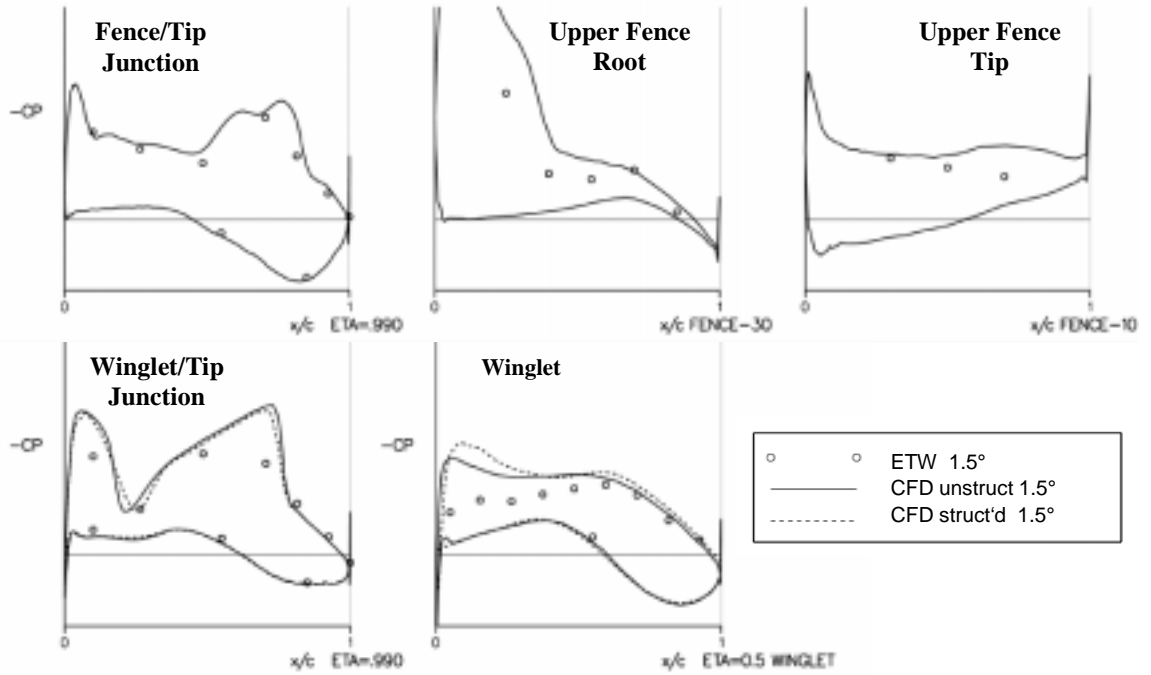


Fig. 12 Wing Tip High Speed Pressures, WTT & CFD, Mach 0.85, Re 54.2million

V. Novel Tip Device Design Studies

A. Approach

Challenging targets were set for the M-DAW novel device design studies under two scenarios. With a focus on high speed the target was for increased range measured by a 1% reduction in a drag function with no penalty at low speed, relative to a conventional device. With a focus on low speed performance the target was for reduced airport noise, measured by a 2% increase in L/D, with no penalty on aircraft range. Both were to be considered as part of a retrofit. This provided a realistic situation often faced by aircraft manufacturers, avoided the complexities associated with a broad aircraft sizing task and reflected the situation within M-DAW itself where devices were being added to an existing wind tunnel model.

High speed assessments and targets have been measured according to an “Equivalent Drag” function which incorporated various multi-disciplinary trades in a single drag figure. This enabled a quick assessment of overall design issues within what is essentially an aerodynamic project, though final assessments will include a more complete analysis of implications for the aircraft as a whole. The terms of the “Equivalent Drag” function are given in equation 1 below.

$$\Delta C_{Dequiv} = \Delta C_{Dest} + \Delta C_{Dtrim} + \Delta C_{Dwrbm} + \Delta C_{Dweight} + \Delta C_{Dmech} \quad (1)$$

The first term C_{Dest} covers the usual aerodynamic drag increments comprising induced drag, profile drag, and wave drag. The second term uses relevant industrial trade information to establish a trim drag term. It is worth noting that whilst a tip device may give large increases in pitching moment the potential trim penalties are usually more than compensated for by the change in the wing drag polar. Thus it is possible for a tip device to be beneficial in terms of trim drag, though the actual magnitude of the difference is likely to be negligible. The third term C_{Dwrbm} relates the increase in wing bending to drag through an approximate weight relationship and can be the most dominant term in the function. The trade used is based on the incremental bending moment at the wing root taking this as indicative of wing weight. The approach is approximate. A focus on the wing root can become misleading and the spanwise change in bending moment must also be monitored during design work. The final two terms account for the additional weight of the tip device itself and the weight of any additional mechanisms and systems should moveable elements be proposed.

Geometric limits were specified at the start of the design task including a minimum span for modifications, representing the limitations inherent in the wind tunnel model components, and a maximum projected span of any device, being that of the large canted winglet.

B. Current Results

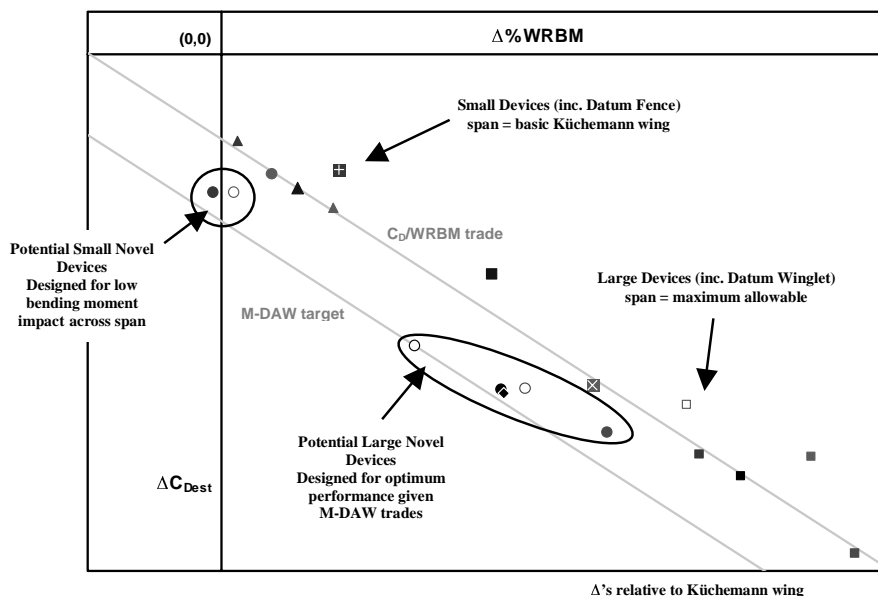


Fig. 13 High Speed Analysis of M-DAW Tip Devices

Initial studies covered a wide range of over 50 devices, including embodiments of devices deemed promising from the State of the Art Review. Investigations included a variety of optimised spiroids, devices with multiple elements such as the split tip and a small c-wing type device, and highly blended shark fin tips. The study also incorporated an extensive parametric optimisation of a conventional winglet using the M-DAW Equivalent Drag function¹⁴. In terms of high speed design the management of increased tip loads has become the dominant theme leading to new classes of novel devices. Figure 13 plots ΔC_{Dest} against incremental bending moment at the design C_L for a selection of devices, data coming from the partners using a variety of design and analysis methods. Note that the wing root bending moment trade line and the associated M-DAW target are plotted relative to the datum fence. Evident are two classes of device: small devices designed for minimal bending moment impact and providing improvements relative to the conventional fence, and a larger set of devices exhibiting a better trade between drag and bending moment relative to the same span large winglet. The dependency on a given set of trades is clear and thus the specific aircraft context to which a device may be applied will determine the preferred solution. It is also important to note that the focus on wing root bending moment is a simplification. The most promising devices are being studied in greater depth, including aeroelastic calculations to establish a better understanding of the impact on wing weight.

Selected devices have also been assessed at low speed. Figure 14 plots the increment in L/D provided by the datum large winglet and two embodiments of a large novel device, assessed with a simple lifting line based design tool validated using the M-DAW test data. The optimisation at high speed has resulted in some loss of performance at low speed conditions in this case. In addition the novel devices have slightly increased local loads relative to the

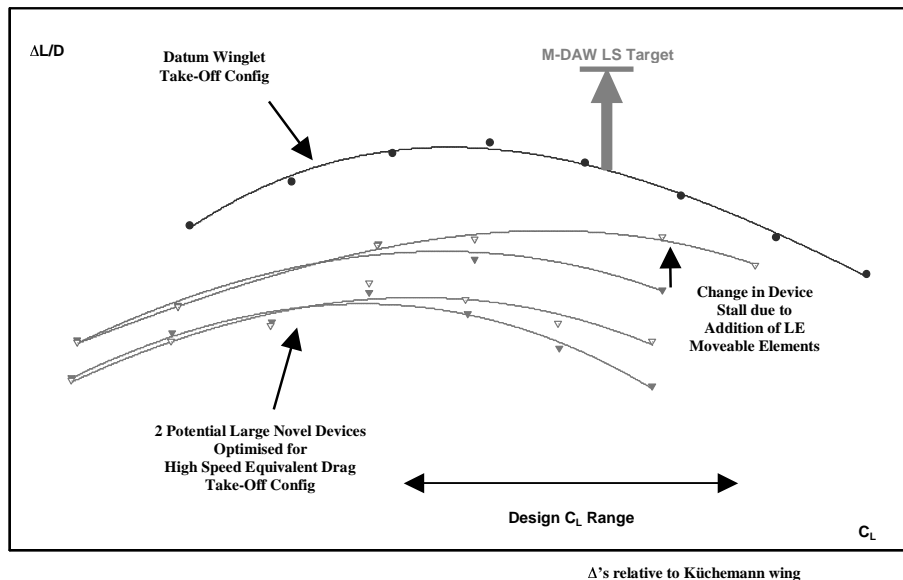


Fig. 14 Low Speed Analysis of M-DAW Tip Devices

datum winglet and experience flow separation at a lower wing C_L . As part of the M-DAW study leading edge devices were applied to selected novel devices to improve the low speed behaviour. It can be seen that the drag benefit of the novel devices persists to higher C_L 's due to delayed stall characteristics. In parallel to the study of moveable elements, fixed section design work has achieved similar benefits for one of the novel devices without the need for moveable devices.

C. Future plans

The promising devices noted above are undergoing further analysis, focusing particularly on their low speed performance and aeroelastic behaviour. Additional studies have also developed approaches for basic tip shaping, confirming the type of design guidelines noted by Hoerner. It is hoped to further develop the M-DAW novel devices to incorporate some of these guidelines. A single device is to be selected from the design work and will be wind tunnel tested at high Reynolds number late in 2005. The second phase test campaign will build on the data and techniques already established and described above at both high and low speed.

VI. Conclusions

A significant data set detailing the performance and characteristics of two conventional wing tip devices has been generated, including extensive pressure measurements and innovative wake measurements. The data has confirmed much of the understanding of tip device aerodynamics, has been used for extensive CFD validation and has provided a state of the art performance standard against which a novel device design exercise is to be judged. The targets set for a novel device refer back to this performance standard. Indications are that the high speed target may be achieved whilst the low speed target is extremely challenging.

To date, design exercises have achieved advances in the capability to manage wing tip loads to provide drag improvements with reduced structural weight penalties. Following these successes a second phase of test campaigns is now likely.

Acknowledgments

The project brings together major European airframe manufacturers (Airbus and Alenia), to address the industrial objectives in a collaborative research project together with four national aerospace research centres (DLR,

NLR, ONERA and QinetiQ), two suppliers of European wind tunnel test facilities (ETW and DNW), and three Universities (Manchester, Warsaw and Braunschweig).

The work and successes here reported are a result of the activities of all partners. It is led by Airbus UK and part funded by the European Commission.

The significant achievements in the use of the DGV technique in ETW were due in no small part to the cooperation and efforts of DLR, ETW and ONERA. DLR developed the technique and equipment for use in ETW. ETW provided support and bore the risk in testing the seeding method. ONERA developed the approach to data analysis and collated the recommendations for future tests. The partners continue to develop the system and its application in ETW in preparation for the final demonstration test of a novel device.

References

- ¹ IPCC, Aviation and the Global Atmosphere, April 1999, <http://www.grida.no/climate/ipcc/aviation/index.htm>
- ² ACARE, Strategic Research Agenda, Oct 2002, <http://www.acare4europe.org>
- ³ M-DAW, Modelling and Design of Advanced Wing tip devices, European 5th Framework G4RD-CT-2002-00837, Oct 2002
- ⁴ Rudolph P. K. C., Boeing, Seattle, US Patent for “High Taper Wing Tip Extension”, No. 5,039,032, filed 19 May 1989
- ⁵ Herrick L. L. et al, Boeing, Seattle, US Patent for “Blunt Leading Edge Raked Wingtips”, No. 6,089,502, filed 12 Jun 1998
- ⁶ Vogt R., US Patent for “Twisted Wing Tip Fin”, No. 2,576,981, filed 1951
- ⁷ Whitcomb R. T., A Design Approach And Selected Wind-Tunnel Results At High Subsonic Speeds For Wing-Tip Mounted Winglets, NASA TN D-8260, 1976
- ⁸ Heller G., Fairchild Dornier, Wessling, Germany, US Patent for “Wing Tip Extension for a Wing”, No. 6,722,615, filed 5 Apr 2002
- ⁹ Jupp J. A., Rees P. H., British Aerospace, London, US Patent for “Aircraft Wing and Winglet Arrangement”, No. 4,714,215, filed 12 Jun 1986
- ¹⁰ Gratzler, L. B., Seattle, US Patent for “Spiroid Tipped Wing”, No. 5,102,068, filed 25 Feb 1991
- ¹¹ Hugues, C., Vitry sur Seine, France, European Patent for “Cylindrical Wing Tip with Helical Slot”, No. WO 02/083497, filed 11 Apr 2001
- ¹² White P., Gibson T., Exploitation by Airbus of High Reynolds Number Test Capabilities in the European Transonic Wind tunnel, AIAA 2004-0768
- ¹³ Willert C. et al, On the Development of Planar Laser Velocimetry Techniques for Cryogenic Wind Tunnels, 5th ISPIV Sept 2003, Paper 3122
- ¹⁴ Büscher A., Streit T., Two-Point-Design of Nonplanar Lifting Configurations Using a Databased Aerodynamic Prediction Tool, DGLR Jahrbuch, Vol. I, pp. 319-327, 2004